Scilight

Highlights in High-Energy Physics
https://www.sciltp.com/journals/hihep

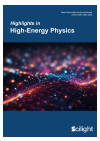

Review

The Discovery of the W and Z Bosons at the CERN Proton-Antiproton Collider

Luigi Di Lella

Physics Department, University of Mainz, 55122 Mainz, Germany; Luigi.Di.Lella@cern.ch

How To Cite: Di Lella, L. The Discovery of the W and Z Bosons at the CERN Proton-Antiproton Collider. *Highlights in High-Energy Physics* **2025**, *1*(1), 8. https://doi.org/10.53941/hihep.2025.100008.

Received: 5 April 2025
Revised: 26 June 2025
Accepted: 29 June 2025
Published: 30 June 2025

Abstract: This article describes the scientific and technical achievements that led to the discovery of the weak intermediate vector bosons, $W^{\pm}$ and Z, from the original proposal to modify an existing high-energy proton accelerator into a proton-antiproton collider and its implementation at CERN, to the design, construction and operation of the detectors which provided the first evidence for the production and decay of these two fundamental particles.

Keywords: UA1; UA2; W and Z discovery

1. Introduction

The first experimental evidence for the existence of the weak neutral Z boson, as predicted by the electro-weak theory formulated in the 1960s, was obtained in 1973 with the discovery of the Neutral Currents (NC). Those were neutrino interactions yielding only visible hadrons as final products. They were explained as resulting from the process $\nu_\mu(\bar{\nu}_\mu) + N \rightarrow \nu_\mu(\bar{\nu}_\mu) +$ hadrons, mediated by the exchange of a massive virtual particle, the neutral mediator of the weak interaction, the Z^{o}. Within the framework of the electroweak theory, the measurement of the cross-section ratio between the NC and the CC (Charged – Current) interactions, $\nu_\mu(\bar{\nu}_\mu) + N \rightarrow \mu^-(\mu^+) +$ hadrons, provided a rough determination of the masses of the two weak bosons. The W mass was predicted to be in the range 60 to 80 GeV/c^2 , while the estimate for the Z was a value between 75 and 92 GeV/c^2. Both values were too large to make possible the production of such heavy states with the accelerators available at that time.

The idea suggested by Rubbia, Cline and McIntyre [1] in 1976 changed completely the scenario. They proposed to transform an existing hadron accelerator in a proton-antiproton collider. The aggressive approach would have allowed to achieve collision energies above the threshold for W and Z production with a quick and relatively modest investment. The new scheme was proposed both to Fermilab and CERN, but it was approved only by this latter laboratory. The SPS, Super Proton Synchrotron accelerator, was transformed in a proton-antiproton collider reaching $\sqrt{s} = 540$ GeV in July 1981. At the end of 1982 it was possible to observe the first leptonic decays of the W, a few months later, in spring 1983 also a handful of leptonic decays of the Z were observed.

In this article, the 1973 discovery of NC neutrino interactions is briefly described (Section 2). Section 3 presents the conception, construction and operation of the CERN $p\bar{p}$ collider. It is followed by the description of the two experiments, UA1 and UA2, of the W and Z discovery, and of the measurement of their properties (Sections 4 and 5).

2. The Discovery of Neutral-Current Neutrino Interactions

In the 1960s, high-energy neutrino beam experiments frequently observed events in which only hadronic activity was detected in the final state. These events were interpreted as resulting from interactions of neutrons, which were produced in ν_μ or $\bar{\nu}_\mu$ charged-current interactions occurring near the downstream end of the shielding. In such cases, the associated muon escaped detection—typically due to its trajectory or energy—while the secondary neutron entered the detector and initiated a hadronic interaction [2].

In 1964 André Lagarrigue proposed to build a large-volume bubble chamber filled with heavy liquid, to be installed on the neutrino beam from the CERN 26 GeV Proton Synchrotron (PS). This chamber, named Gargamelle, was built in Saclay and installed at CERN in 1970. It had a cylindrical volume 4.8 m long, with a diameter of 1.8 m,

located between two magnetic coils which provided a horizontal magnetic field of 2 T orthogonal to the beam axis (Figure 1). It was filled with liquid Freon-13, whose density is about 1.5 g/cm^3 (in its boiling point at –81.4 C or 191.75 K and atmospheric pressure), a radiation length of 11 cm, and a mean nuclear interaction length of 78 cm. Data-taking started in 1971, using ν_μ and ($\bar{\nu}_\mu$) beams with energy distributions between 1 and 10 GeV.

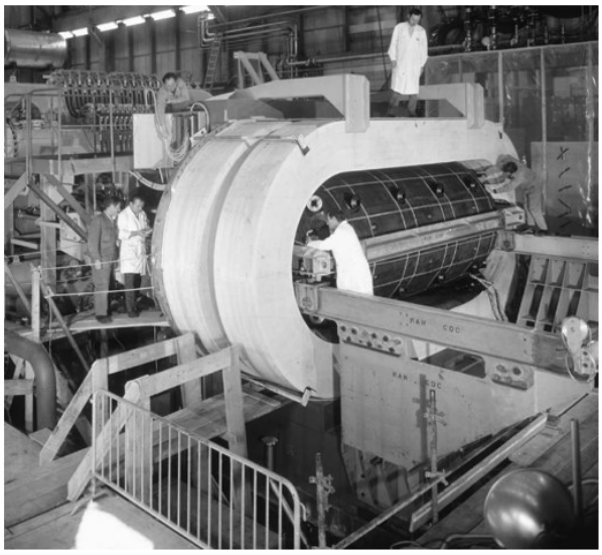

Figure 1. The Gargamelle body installed inside the magnetic coils.

The first hint for the existence of NC interactions was obtained in 1971 by the observation of an event consisting of a single electron only during a run with a $\bar{\nu}_\mu$ beam [3]. In this event, shown in Figure 2, the electron had an energy of 385 ± 100 MeV and was emitted at an angle of $1.4^\circ \pm 1.4^\circ$ with respect to the beam axis. The most probable explanation of this event was $\bar{\nu}_\mu$ elastic scattering on an atomic electron, $\bar{\nu}_\mu + e^- \to \bar{\nu}_\mu + e^-$, which, to first order, could only be explained by the exchange of a neutral vector boson, as predicted by the electroweak theory. The background from CC processes involving incident ν_e or $\bar{\nu}_e$, a beam contamination of less than 1%, was estimated to amount to 0.03 ± 0.02 events.

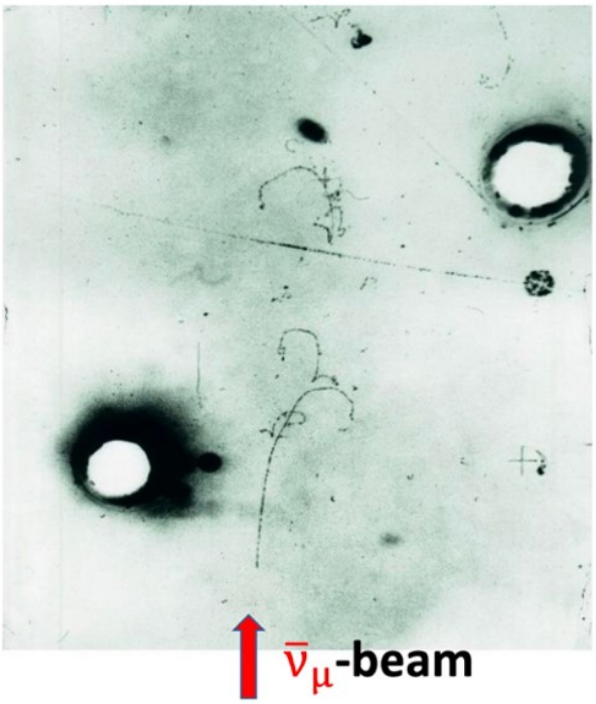

Figure 2. A single-electron event observed in Gargamelle during a $\bar{\nu}_\mu$ run in 1971.

The background from neutron interactions in events with final states consisting of hadrons only was studied by using CC ν_μ ($\bar{\nu}_\mu$) interactions occurring near the chamber entrance, with the outgoing muon clearly identified. The

total energy measured in the neutron interactions was typically less than 500 MeV, and the longitudinal distribution along the chamber was consistent with the expected neutron mean free path. However, the ν_μ and $\bar{\nu}_\mu$ interactions with only visible hadrons having a total energy of more than 1 GeV had a uniform longitudinal and radial distribution in the chamber [4], similar to the CC events with a visible muon, as expected for NC interactions (see Figure 3). The ratio NC/CC was measured to be 0.21 ± 0.03 for ν_μ, and 0.45 ± 0.09 for $\bar{\nu}_\mu$, both compatible with the same value of the weak mixing angle, $\sin^2 \theta_W$, in the range 0.3 to 0.4. A typical neutrino interaction with only hadrons in the final state is shown in Figure 4. In this event all three tracks are identified as hadrons from their interactions in the chamber.

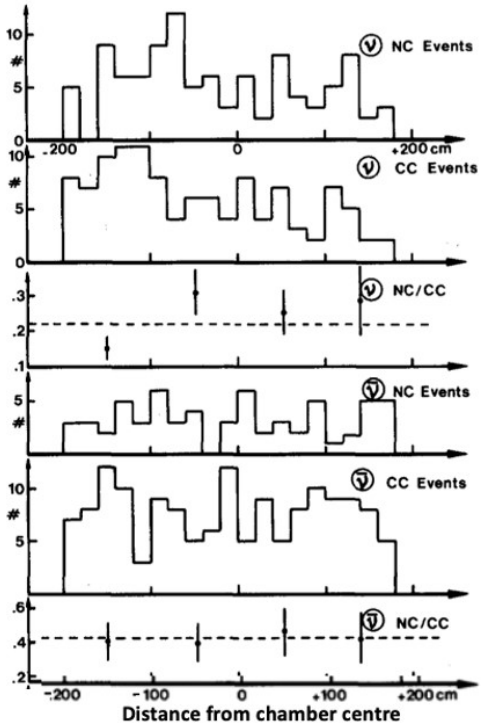

Figure 3. Event distributions and NC/CC ratios vs. distance from chamber centre [4].

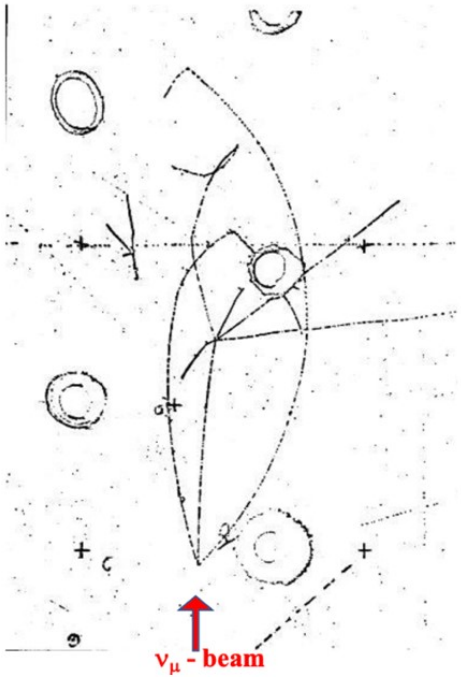

Figure 4. A neutrino interaction with three final-state hadrons and no muon.

3. The CERN $p\bar{p}$ Collider

The conception, construction and operation of the CERN proton-antiproton collider was a great achievement in itself. It is useful, therefore, to give a short description of this facility.

The production of W and Z bosons at a $p\bar{p}$ collider is expected to occur mainly as the results of quark-antiquark annihilation: $\bar{d}u \to W^+$; $\bar{u}d \to W^-$; $u\bar{u} \to Z$; $d\bar{d} \to Z$. Because 50% of the momentum of a high-energy proton is carried by three valence quarks, and the remainder by gluons, a valence quark carries, on average, about $1/6$ of the proton momentum. As a consequence, W and Z production should require a $p\bar{p}$ collider with a total center-of-mass energy equal to about six times the boson masses, or 500–600 GeV.

The detection of $Z \to e^+e^-$ decays determines the minimal collider luminosity: the cross-section for inclusive Z production at ∼600 GeV is ∼1.6 nb, and the fraction of $Z \to e^+e^-$ decays is ∼3%, hence a luminosity $L = 2.5 \times 10^{29}\,\mathrm{cm}^{-2}s^{-1}$ would give an event rate of ∼1 per day. To achieve such luminosities one would need an antiproton source capable of delivering daily $\sim 3 \times 10^{10}$ $\bar{p}$ distributed in few (3–6) tightly collimated bunches within the angular and momentum acceptance of the CERN SPS.

The 26 GeV CERN Proton Synchrotron (PS) was capable of producing antiprotons at the required rate. Each PS pulse accelerated approximately 10^{13} protons, delivered every $2.4\,\mathrm{s}$ to the antiproton production target. About 7×10^6 antiprotons with a momentum of $3.5\,\mathrm{GeV/c}$ were produced at 0° within a solid angle of 8×10^{-3} sr and a momentum spread of $\Delta p/p = 1.5\%$. While this yield was sufficient in number, the resulting antiprotons occupied a phase-space volume more than $\geq 10^8$ times too large to be accepted by the SPS, even after acceleration to its injection energy of $26\,\mathrm{GeV}$. To overcome this, the phase-space density of the antiproton beam had to be increased by at least a factor of 10^8 before injection into the SPS. This process, known as cooling, reduces the spread of particle velocities—akin to compressing a hot gas—when viewed in the center-of-mass frame of the antiproton bunch.

The CERN collider project used the technique of stochastic cooling, invented by S. van der Meer in 1972 [5,6]. The developed principle is known as stochastic cooling and is illustrated in Figure 5. Let us consider, for simplicity, the horizontal "betatron" oscillations. If a transverse pick-up detector is located at the maximum amplitude of the oscillation, using fast processing electronics and transmission cables, it is possible to generate a signal triggering a transverse kicker exactly when the particle, whose orbit must be corrected, is passing by.

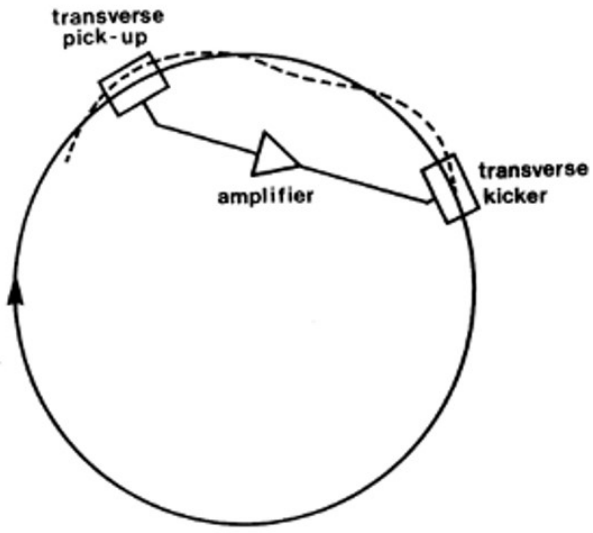

Figure 5. Cooling of a single particle (dotted line) horizontal oscillation.

Following the success of the so-called Initial Cooling Experiment (ICE) [7], which provided the experimental demonstration that stochastic cooling could indeed achieve the required increase of $\bar{p}$ phase-space density, the CERN proton-antiproton collider project was approved on May 28, 1978. For the CERN collider, stochastic cooling was achieved in a purpose-built machine called Antiproton Accumulator (AA), which included several independent cooling systems to cool both horizontal and vertical oscillations, and also to decrease the beam momentum spread (cooling of longitudinal motion), by using pick-up electrodes which provided signals proportional to Δp. The AA is a large aperture magnetic ring. A picture of the AA during construction is shown in Figure 6. Figure 7 illustrates the operation of cooling and accumulation of a $\bar{p}$ stack in the AA.

Figure 6. View of the Antiproton Accumulator during construction.

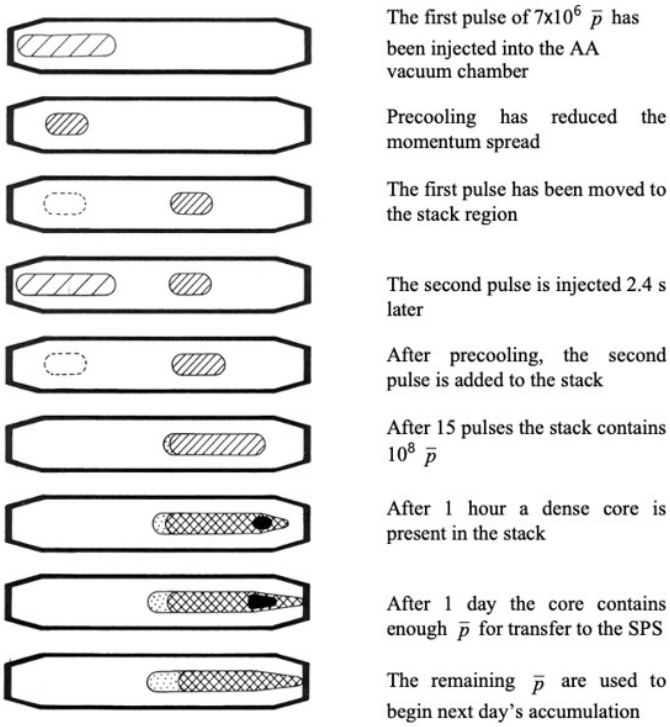

Figure 7. Schematic sequence illustrating antiproton cooling and accumulation in the AA [1].

Consecutive PS cycles achieved beam injection into the SPS, when AA accumulated a sufficiently dense $\bar{p}$ stack. Firstly, three proton bunches (six after 1986), each containing $\sim 10^{11}$ protons, are accelerated to 26 GeV in the PS and injected into the SPS (see Figure 8). Then three $\bar{p}$ bunches (six after 1986), of typically $\sim 10^{10}$ each, are extracted from the AA and injected into the PS. Here they are accelerated to 26 GeV in a direction opposite to that of the protons, and then injected into the SPS. The relative injection timing of the bunches is controlled with a precision of ~ 1 ns to ensure that bunch crossing in the SPS occurs in the centre of the detectors.

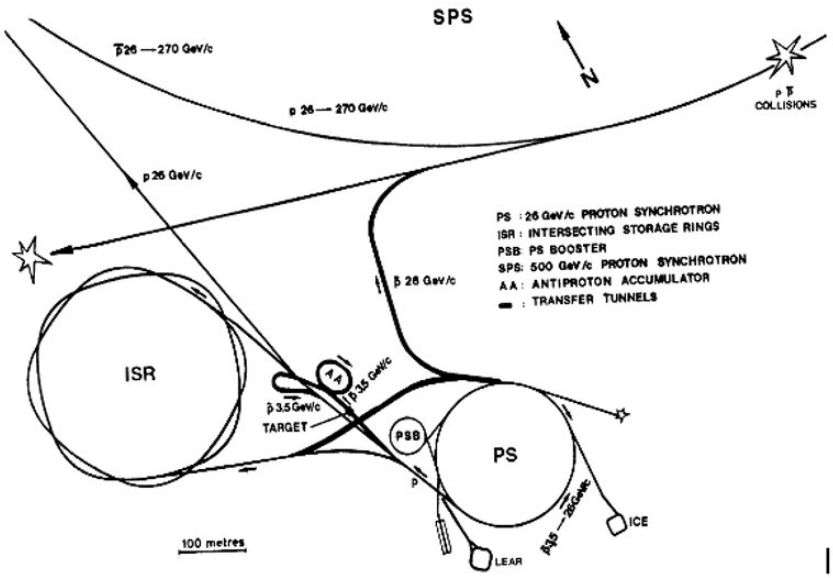

Figure 8. Layout of the three machines initially involved in the operation of the CERN $p\bar{p}$ collider: the PS, the AA, the SPS and the interconnecting transfer lines.

In 1987, to increase the luminosity of the machine, the source of antiprotons was upgraded. A second ring, the Antiproton Collector (AC) which had a much larger acceptance was built around the AA. As a result the stacking rate for antiprotons was increased by a factor of ~ 10. The main collider parameters and their evolution with time are shown in Table 1. The CERN proton-antiproton collider completed its operations in 1990 and was shut-down at the end of the year.

Table 1. CERN proton-antiproton collider operation, 1981–1990.

Year	Collision Energy (GeV)	Peak luminosity ($\mathbf{cm^{-2}\,s^{-1}}$)	Integrated luminosity ($\mathbf{cm^{-2}}$)
1981	546	$\sim 10^{27}$	2×10^{32}
1983	546	5×10^{28}	1.5×10^{35}
1984–1985	630	3.9×10^{29}	1.0×10^{36}
1987–1990	630	3×10^{30}	1.6×10^{37}

4. The Discovery of the W and Z Bosons

Since the SPS is built in an underground tunnel at an average depth of $\sim$100 m, the project also required the excavation of underground experimental areas to house the detectors. The first experiment, named UA1 for "Underground Area 1", was soon approved on 29 June 1978. UA2, the second experiment, followed a few months later and was approved at the end of the year.

4.1. The UA1 Experiment

The UA1 experiment is a general-purpose magnetic detector with an almost complete 4π coverage [8]. Figure 9 shows a schematic view of the detector. The magnet is a dipole with a horizontal field of $0.7\,\mathrm{T}$ over a volume of $7 \times 3.5 \times 3.5\,\mathrm{m}^3$, perpendicular to the beam axis and produced by a warm aluminium coil to minimize absorption.

The magnet contained the central track detector, which was a system of drift chambers filling a cylindrical volume $5.8\,\mathrm{m}$ long with a $2.5\,\mathrm{m}$ diameter, reconstructing charged particle trajectories down to polar angles of $\sim 6^\circ$ with respect to the beams. Tracks were sampled approximately every centimetre and could have up to 180 hits. This detector, at the cutting edge of technology in those days, was surrounded by electromagnetic and hadronic calorimeters down to 0.2° to the beam line. This "hermeticity", as it was called later, turned out to be very effective to reconstruct undetected neutrinos from $W \to e\nu$ decay, and also to search for possible new, as yet undiscovered neutral particles escaping direct detection. It became one of the basic features of all general-purpose detectors at the next-generation e^+e^- and hadron colliders (LEP, the Fermilab $p\bar{p}$ collider and the LHC).

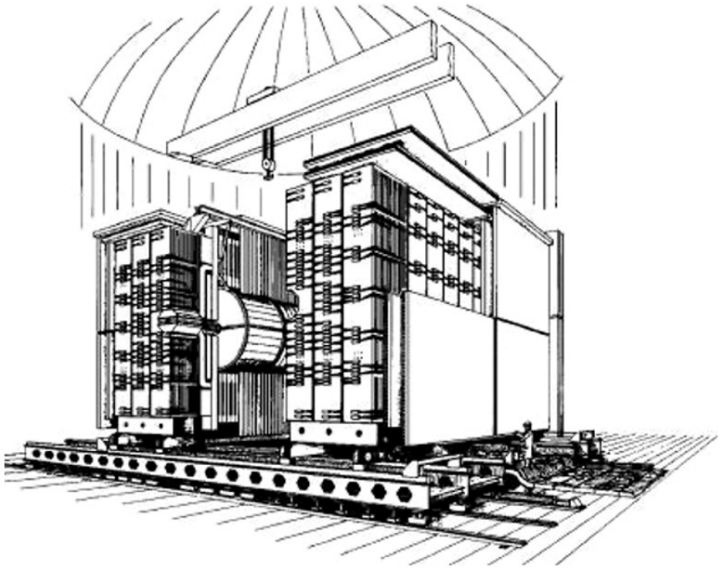

Figure 9. View of the UA1 detector with the two magnet halves opened up.

Electromagnetic calorimeters are installed inside the magnet and they consist of scintillators interleaved with sheets of lead to form a multi-layered sandwich. The central region is organised in two cylindrical half-shells surrounding the tracker, each subdivided into 24 elements ("gondolas"). The geometrical coverage is $180°$ in ϕ and 24 cm along the beam line. The total thickness of the calorimeter is 26.4 radiation lengths (X_0). Two similar structures were present at smaller angles to the beam line, each consisting of 32 radial sectors. The energy resolution for electrons was measured to be $\sigma(E)/E = 0.15/\sqrt{E}$ (E in GeV). A 40 GeV electron could therefore be measured with a typical ±2.5% energy resolution.

The hadronic calorimeter was built by inserting scintillator planes into the laminated structure of the magnet return yoke, and two iron walls located symmetrically at the two ends of the magnet. The hadron calorimeter was segmented into 450 independent cells.

A complex system of drift tubes surrounding the magnet joke, provided information to detect muons and measure their momentum. Muon detectors, consisting of systems of drift tubes, surrounded the magnet yoke. The typical momentum resolution for a 40 GeV/c muon track was ±20%.

A picture of UA1 during the assembly phase is shown in Figure 10.

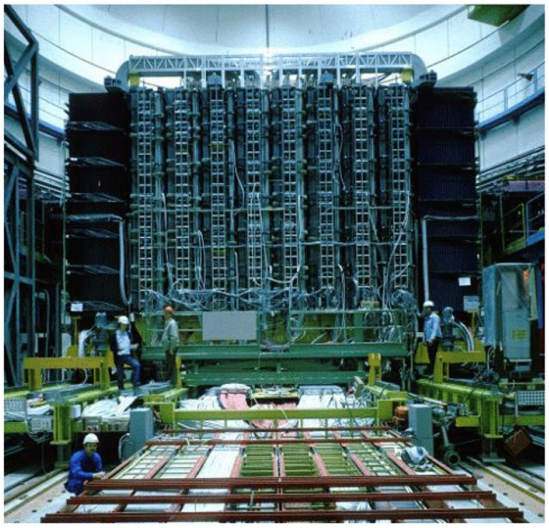

Figure 10. The UA1 detector during assembly.

4.2. The UA2 Experiment

UA2 was not designed as a general-purpose detector, but rather optimized for the detection of electrons from W and Z decays. The emphasis was on highly granular calorimetry with spherical projective geometry, which was well adapted also to the detection of hadronic jets.

Figure 11 shows the layout of the UA2 detector for the collider runs between 1981 and 1985. The central region contained a "vertex detector", which consisted of various types of cylindrical tracking chambers. A "preshower" counter, located just behind the last chamber and consisting of a tungsten cylinder followed by a multi-wire proportional chamber, was crucial for electron identification. The vertex detector was surrounded by the central calorimeter, which covered the full azimuth and was subdivided into 240 independent cells, each subtending the angular interval $\Delta\theta \times \Delta\phi = 10^\circ \times 15^\circ$ and consisting of an electromagnetic (Pb-scintillator) and a hadronic (Fe-scintillator) section. The calorimeter energy resolution for electrons was $\sigma(E)/E = 0.14/\sqrt{E}$ (E in GeV), and was $\sim$10% for an 80 GeV hadron in the central calorimeters. There was no magnetic field in this region.

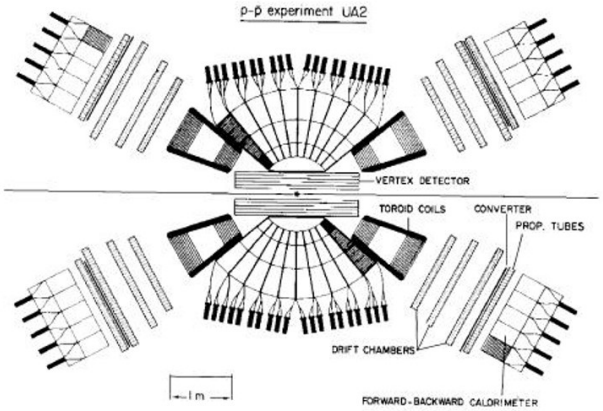

Figure 11. Sketch of the UA2 detector in the 1981–1985 configuration.

Twelve azimuthal sectors composed the two forward detectors. Each sector consisted of tracking chambers and an electromagnetic calorimeter equipped with a "preshower" detector. Individual coils generated a toroidal magnetic field in the forward/backward regions. The UA2 detector had no coverage for muons. The collaboration gathered, initially, about 60 scientists coming from three research institutes, CERN, Orsay and Saclay, and three universities, Bern, Copenhagen, Pavia. A picture of UA2 during assembly is shown in Figure 12.

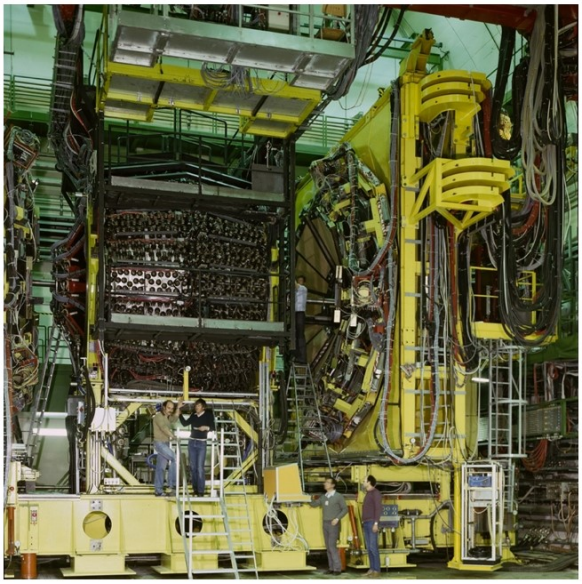

Figure 12. The UA2 detector in its 1981–1985 configuration.

4.3. Discovery of the W Boson

The dominant decay mode of the W boson is to quark-antiquark pairs, i.e. hadronic jets. Unfortunately, this decay mode, that accounts for about 70% of the branching fraction, is overwhelmed by QCD processes yielding an irreducible two-jet background. This is the reason why both UA1 and UA2 focused on the leptonic decay of the W. Both experiments were optimised to detect high p_T isolated electrons produced in the decay $W^\pm \to e^\pm \nu_e(\bar{\nu}_e)$ and high missing transverse due to the neutrino. UA1 was able to identify also muons produced in the decay

$W^{\pm} \to \mu^{\pm}\nu_{\mu}(\bar{\nu}_{\mu})$.

The signal from $W \to e\nu_e$ decay is expected to have the following features:

- the presence of a high transverse momentum (p_T) isolated electron;
- peak in the electron p_T distribution at $m_W/2$, where m_W is the W mass;
- the presence of high missing transverse momentum from the undetected neutrino.

It is important to note that the longitudinal component of missing momentum (along the beam axis) cannot be reliably measured at hadron colliders. This is because a significant number of high-energy secondary particles from the hadrons are produced at very small polar angles relative to the beam direction. These particles travel down the beam pipe and are not intercepted by the detector, as they remain inside the vacuum system of the accelerator. As a result, any momentum they carry in the longitudinal direction is not accounted for, making it impossible to reconstruct the total momentum along the beam axis. Only the transverse component of missing momentum can be inferred from the measured imbalance in the detector's transverse plane.

The missing transverse momentum vector ($\vec{p}_T^{\,miss}$) is defined as

$$\vec{p}_T^{\,miss} = -\sum_{cells} \vec{p}_T \tag{1}$$

where $\vec{p}_T$ is the transverse component of a vector associated to each calorimeter cell, with direction from the event vertex to the cell center and length equal to the energy deposition in that cell, and the sum is extended to all cells with an energy deposition larger than zero. For UA1 events with final-state muons, the muon transverse momenta are also added. In an ideal detector with perfect measurement, and assuming a final-state neutrino is the only undetected particle, momentum conservation implies that the $\vec{p}_T^{\,miss}$ corresponds exactly to the transverse momentum of the neutrino.

Figure 13 shows the $|\vec{p}_T^{\,miss}|$ distribution, as measured by UA1 from the 1982 data[9]. There is a component decreasing approximately as $|\vec{p}_T^{\,miss}|^2$, due to the effect of calorimeter resolution in events without significant $\vec{p}_T^{\,miss}$, followed by a flat component due to events with genuine $\vec{p}_T^{\,miss}$. Six events with high $\vec{p}_T^{\,miss}$ in the distribution of Figure 13 contain a high p_T electron. The $\vec{p}_T^{\,miss}$ vector in these events is almost back-to-back with the electron transverse momentum vector, as shown in Figure 14. These events are interpreted as due to $W \to e\nu_e$ decay. This result was first announced at a CERN seminar on January 20, 1983. Figure 15 shows the graphics display of one of these events. A fit to the distribution of these events using m_W as a free parameter gives $m_W = 81 \pm 5\,\text{GeV/c}^2$.

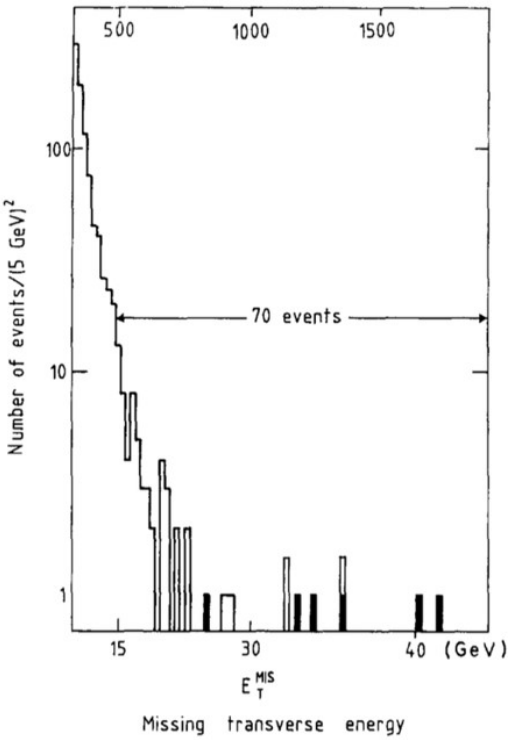

Figure 13. UA1 distribution of the missing transverse momentum (called E_T^{MIS} in this plot) for equal bins of $(E_T^{MIS})^2$. The events shown as dark areas in this plot contain a high p_T electron.

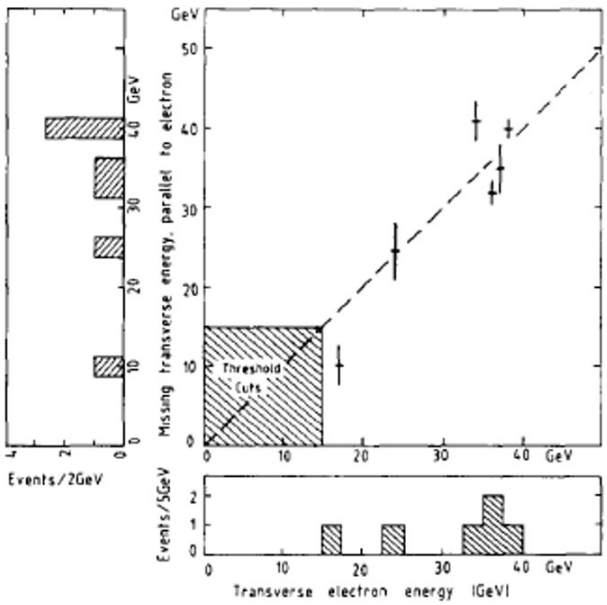

Figure 14. UA1 scatter plot of all the events from the 1982 data which contain a high $-$ p_T electron and large $\vec{p}_T^{miss}$. The abscissa is the electron p_T and the ordinate is the $\vec{p}_T^{miss}$ component antiparallel to the electron $\vec{p}_T$.

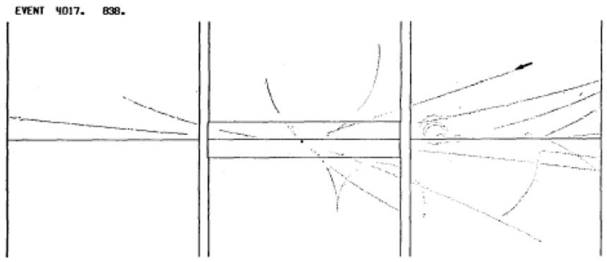

Figure 15. Display of a UA1 $W \to e\nu_e$ event. The arrow points to the electron track.

The results from the UA2 search for $W \to e\nu_e$ events[10] were presented at a CERN seminar on the day after the UA1 presentation. Six events containing an electron with $p_T > 15$ GeV/c were identified among the 1982 data. Figure 16a shows the distribution of the ratio between $|\vec{p}_T^{miss}|$ and the electron p_T for these events, while Figure 16b displays the electron p_T distribution for the events with $|\vec{p}_T^{miss}|$ larger than 80% of the electron p_T (four events). These events have the properties expected from $W \to e\nu_e$ decay. A fit to the distribution of these events using m_W as a free parameter gives $m_W = 80^{+10}_{-6}$ GeV/c^2.

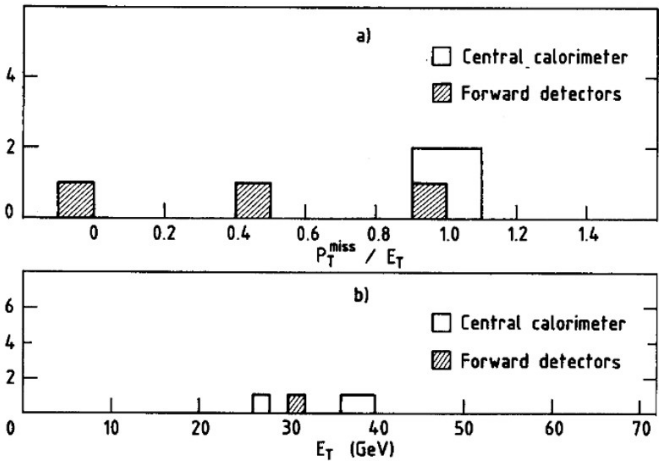

Figure 16. (**a**) Distribution of the ratio between the missing transverse momentum in the event and the electron transverse momentum (called E_T in this plot) for six UA2 events containing an electron with $E_T > 15$ GeV; (**b**) Electron transverse momentum distribution for the four events with the highest $|\vec{p}_T^{miss}|/E_T$ ratio.

4.4. Discovery of the Z Boson

Figure 17 illustrates the search for the decay $Z \to e^+e^-$ in UA1[11]. The first step of the analysis requires the presence of two calorimeter clusters consistent with electrons and having a transverse energy $E_T > 25\,\text{GeV}$. Among the data recorded during the 1982–1983 collider run, 152 events are found to satisfy these conditions. The next step requires the presence of an isolated track with $p_T > 7\,\text{GeV/c}$ pointing to at least one of the two clusters. Six events satisfy this requirement, showing already a clustering at high invariant mass values, as expected from $Z \to e^+e^-$ decay. Of these events, four are found to have an isolated track with $p_T > 7\,\text{GeV/c}$ pointing to each clusters. They are consistent with a unique value of the e^+e^- invariant mass within the calorimeter resolution. One of these events is displayed in Figure 18.

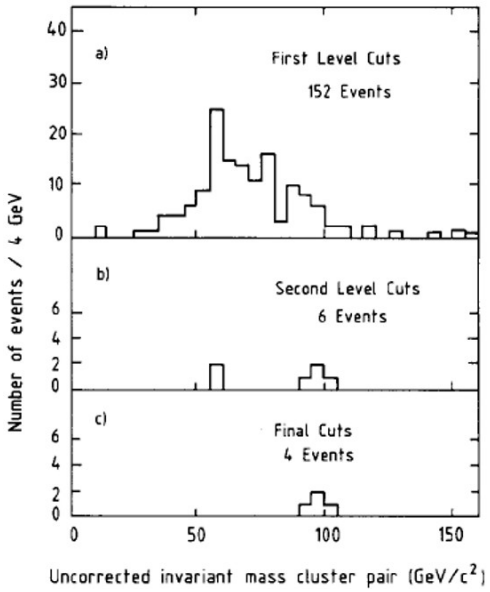

Figure 17. Search for the decay $Z \to e^+e^-$ in UA1 (see text).

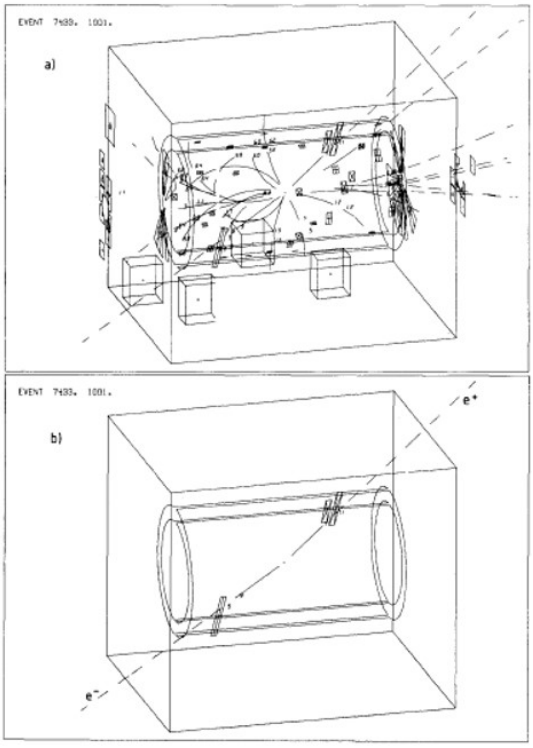

Figure 18. One of the $Z \to e^+e^-$ events in UA1: (**a**) display of all reconstructed tracks and calorimeter hit cells; (**b**) only tracks with $p_T > 2\,\text{GeV/c}$ and calorimeter cells with $E_T > 2\,\text{GeV}$ are shown.

An event consistent with the decay $Z \to \mu^+\mu^-$ was also found by UA1 among the data collected in 1983 [11]. Figure 19 shows the mass distribution of all lepton pairs found by UA1 from the analysis of the 1982–1983 data. The mean of these values is

$$m_Z = 95.2 \pm 2.5 \pm 3.0\,\text{GeV/c}^2 \tag{2}$$

The first uncertainty arises from statistical, while the second originates from the systematic uncertainty associated with the calorimeter energy scale calibration.

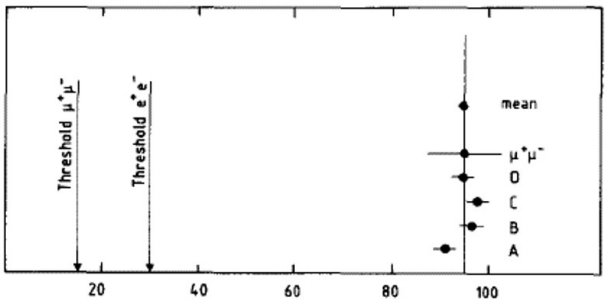

Figure 19. Invariant mass distribution of all lepton pairs detected by UA1 in the 1982–1983 data.

The UA2 search for the decay $Z \to e^+e^-$ among the 1982–1983 data [12] is illustrated in Figure 20. First, pairs of energy depositions in the calorimeter consistent with two isolated electrons and with $p_T > 25\,\text{GeV}$ are selected. Then, an isolated track consistent with an electron (from preshower information) is required to point to at least one of the clusters. Eight events satisfy these requirements: of these, three events have isolated tracks consistent with electrons pointing to both clusters. The weighted average of the invariant mass values for the eight events is

$$m_Z = 91.9 \pm 1.3 \pm 1.4\,\text{GeV/c}^2 \tag{3}$$

where the first error is statistical and the second one originates from the systematic uncertainty on the calorimeter energy scale. The latter is smaller than the corresponding UA1 value because the smaller size of the UA2 calorimeter, and its modularity, allow frequent recalibrations on electron beams of known energies from the CERN SPS.

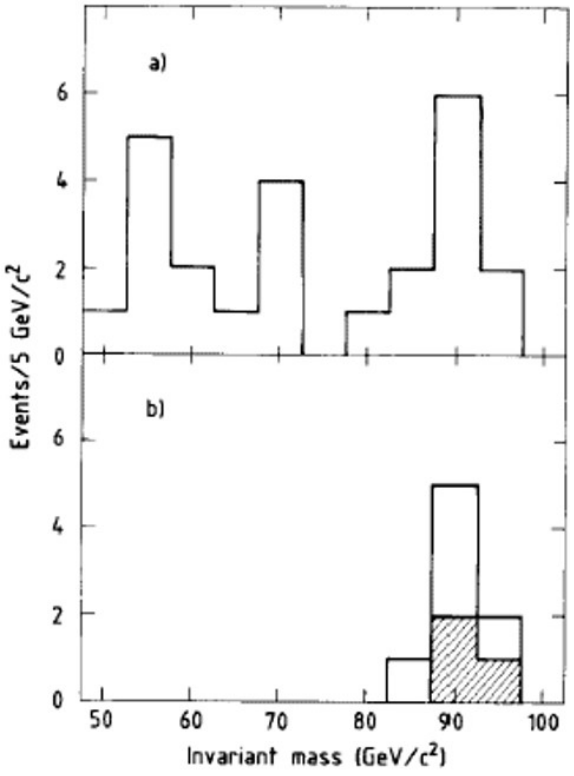

Figure 20. Search for the decay $Z \to e^+e^-$ in UA2 (see text). The shaded area represents the three events with isolated electron tracks pointing to both energy clusters in the calorimeter.

Figure 21 shows the energy deposited in the UA2 calorimeter by a $W \to e\nu$ and by a $Z \to e^+e^-$ event. These distributions exemplify the distinctive topologies of such events, characterized by a substantial deposition of energy within a limited number of calorimeter cells, with minimal or no energy detected in the remaining cells.

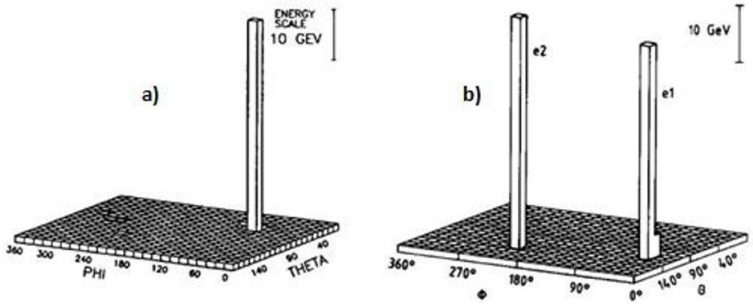

Figure 21. The energy deposited in the UA2 calorimeter for a $W \to e\nu$ (**a**) and a $Z \to e^+e^-$ event (**b**).

5. Physics Results from Subsequent Collider Runs

Following the historical runs in 1982–1983 which led to the discovery of the W and Z bosons, additional runs took place in the following years. In a first phase, up to the end of 1985, with the two detectors basically unchanged, the collider energy was raised from $\sqrt{s} = 540$ GeV to 630 GeV and the peak luminosity doubled. Then, between 1987 and the collider shut-down at the end of 1990, more physics runs took place at higher luminosity (see Section 3, Table 1). The most important results on W and Z physics achieved during these runs are described in the next subsections.

5.1. W and Z Masses and Production Cross-Sections

At the end of 1985, UA1 had recorded 290 $W \to e\nu$, 33 $Z \to e^+e^-$, 57 $W \to \mu\nu$ and 21 $Z \to \mu^+\mu^-$ [13]. As an example, Figure 22 shows the $W \to e\nu$ transverse mass (M_T) distribution, where

$$M_T = \sqrt{2p_T^e p_T^\nu (1 - \cos\phi_{e\nu})} \tag{4}$$

and $\phi_{e\nu}$ is the azimuthal separation between electron and neutrino (the electron transverse momentum is instead by the transverse mass, due to its reduced sensitivity to the transverse momentum of the W boson).

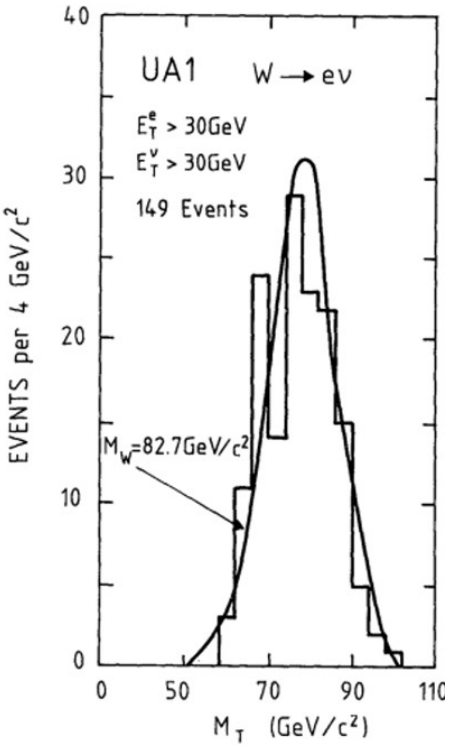

Figure 22. Transverse mass distribution for all 1982–1985 UA1 $W \to e\nu$ events.

Figure 23 shows the invariant mass distribution of all e^+e^- pairs recorded by UA1 during the same period. The W and Z mass values obtained from fits to the distributions of Figures 22 and 23 were

$$m_W = 82.7 \pm 1.0 \pm 2.7\,\text{GeV/c}^2 \quad (5)$$
$$m_Z = 93.1 \pm 1.0 \pm 3.1\,\text{GeV/c}^2 \quad (6)$$

respectively, where the first error is statistical and the second one reflects the uncertainty on the calorimeter energy scale. The W and Z production cross-sections values, multiplied with the corresponding decay branching ratios (BR), as measured by UA1, were

$$\sigma_W\,\text{Br}\,(W \to e\nu) = 630 \pm 50 \pm 100\,\text{pb} \quad (7)$$
$$\sigma_Z\,\text{Br}\left(Z \to e^+e^-\right) = 74 \pm 14 \pm 11\,\text{pb} \quad (8)$$

UA1 has also observed 32 $W \to \tau\nu_\tau$ decays followed by τ hadronic decay [14]. These events appeared in the detector as a highly collimated, low multiplicity hadronic jet approximately back-to-back in azimuth to the $\vec{p}_T^{\,miss}$ vector.

In the same physics runs, from 1982 to 1985, the UA2 experiment had recorded samples of 251 $W \to e\nu$ and 39 $Z \to e^+e^-$ events[15]. The measured properties of these events were in good agreement with the UA1 results. The W and Z mass values, as measured by UA2, were

$$m_W = 80.2 \pm 0.8 \pm 1.3\,\text{GeV/c}^2 \quad (9)$$
$$m_Z = 91.5 \pm 1.2 \pm 1.7\,\text{GeV/c}^2 \quad (10)$$

respectively, where, as usual, the first error is statistical and the second one reflects the uncertainty on the calorimeter energy scale.

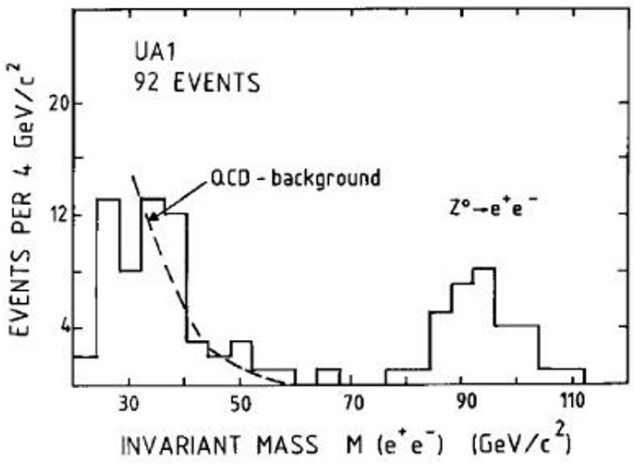

Figure 23. Invariant mass distribution of all 1982–1985 UA1 e^+e^- pairs.

5.2. Charge Asymmetry in the Decay $W \to e\nu$

The angular distribution of the charged lepton in the W rest frame can be written as

$$\frac{dn}{d\cos\theta^*} \propto (1 + q\cos\theta^*)^2 \quad (11)$$

where θ^* is the angle of the charged lepton measured with respect to the W polarization, and $q = -1\,(+1)$ for electrons (positrons). This axis is practically collinear with the incident $\bar{p}$ direction if the W transverse momentum is small.

A complication arises from the fact that the neutrino longitudinal momentum is not measured, and the requirement that the invariant mass of the $e\nu$ pair be equal to the W mass gives two solutions for θ^*. The UA1 analysis[13] retains only those events for which one solution is unphysical (W longitudinal momentum inconsistent with kinematics), and the lepton charge sign is unambiguously determined. Figure 24 shows the distribution of the variable $q\cos\theta^*$ for 149 unambiguous events. The distribution agrees with the expected $(1 + q\cos\theta^*)^2$ form. It must be noted that this result cannot distinguish between V-A and V+A because in the latter case all helicities change sign and the angular distribution remains the same.

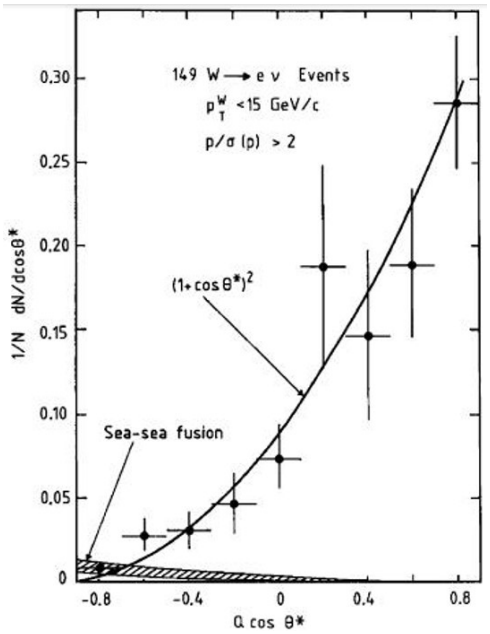

Figure 24. Decay angular distribution for the final UA1 $W \to e\nu$ event sample (see text). The shaded band shows the expected contribution of wrong polarization from the annihilation of a sea quark with a sea antiquark.

5.3. A Test of QCD: The W Boson Transverse Momentum

To lowest order, the W and Z bosons produced by $q\bar{q}$ annihilation are emitted with very low transverse momentum. However, gluon radiation from the initial quarks (or antiquarks) may result in W and Z production with a sizeable transverse momentum, which is equal and opposite to the total transverse momentum of all hadrons produced in association with the intermediate bosons.

Figure 25 shows the distribution of the W transverse momentum, p_T^W, as measured by UA1 [13] using the $W \to e\nu$ event sample. A QCD prediction [16], also shown in Figure 25, agrees with the data over the full p_T^W range. The W bosons produced with high p_T^W are expected to recoil against one or more jets, and such jets are indeed observed experimentally.

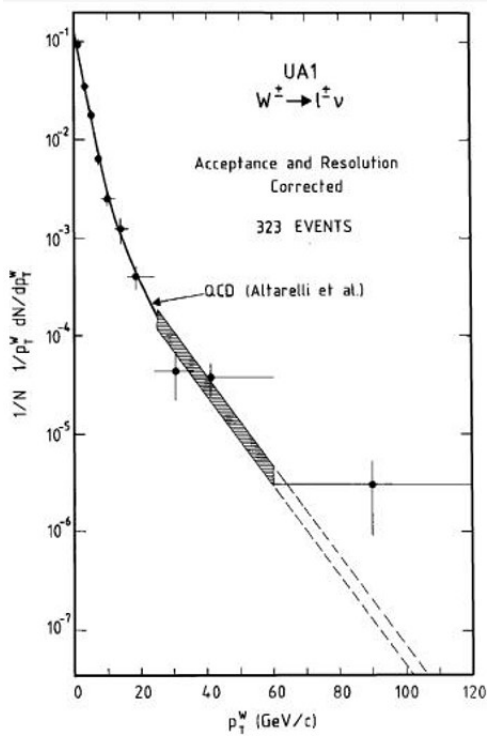

Figure 25. Distribution of p_T^W, as measured by UA1. The curve is a QCD prediction [16]. The shaded band shows the theoretical uncertainty in the region of high p_T^W.

5.4. Precision Measurement of the W to Z Mass Ratio

In view of the last collider runs at higher luminosity (1987–1990, see Section 3, Table 1), the UA2 detector underwent a major upgrade: new segmented calorimeters were installed in the forward regions to improve the hermeticity. The central tracking system was upgraded using silicon pad detectors, scintillating fibres and transition radiation detectors. Figure 26 displays the UA2 layout for the 1987–1988 collider run. University groups from Cambridge, Heidelberg, Milano, Perugia and Pisa joined the collaboration bringing the total number of physicists to about 100.

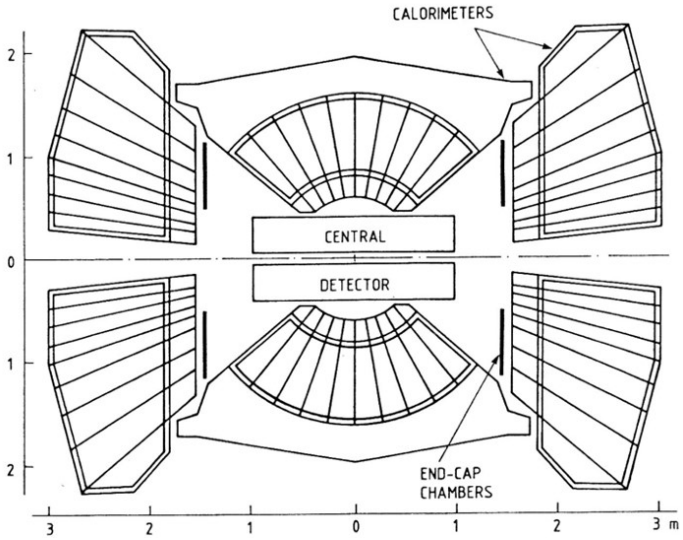

Figure 26. The UA2 detector layout for the 1987–1988 collider run.

From 1988 to 1990, UA2 collected large samples of $W \to e\nu$ and $Z \to e^+e^-$ events.

Figure 27 shows the transverse mass distribution for 2065 $W \to e\nu$ decays with the electron measured in the UA2 central calorimeter [17]. A best fit to this distribution using m_W as a free parameter gives $m_W = 80.84 \pm 0.22\text{GeV/c}^2$ (statistical error only).

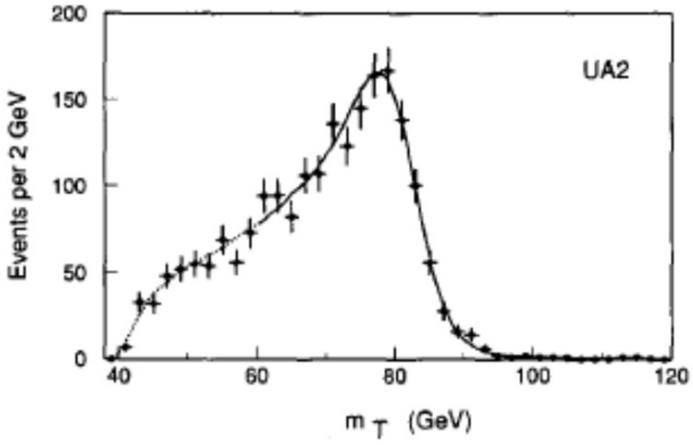

Figure 27. Transverse mass distribution for 2065 $W \to e\nu$ decays (see text). The curve is the best fit to the experimental distribution using m_W as a free parameter.

The measured e^+e^- invariant mass distribution [17] is shown in Figure 28, which displays two spectra: one containing 95 events in which both electrons fall in a fiducial region of the central calorimeter and their energies are accurately measured (Figure 28a); and the other spectrum containing 156 events in which one of the two electrons falls outside the fiducial region of the central calorimeter, resulting in a broader mass resolution (Figure 28b). Best fits to the two spectra give $m_Z = 91.65 \pm 0.34\,\text{GeV/c}^2$ and $m_Z = 92.10 \pm 0.48\,\text{GeV/c}^2$, respectively. The weighted mean of these two values is $m_Z = 91.74 \pm 0.28\,\text{GeV/c}^2$ (statistical error only).

The two independent measurements of m_W and m_Z give

$$\frac{m_W}{m_Z} = 0.8813 \pm 0.0036 \pm 0.0019 \tag{12}$$

where the first error is statistical and the second one is a small systematic uncertainty which takes into account a possible calorimeter non-linearity.

By 1991, a precise measurement of m_Z from LEP experiments had become available [18]

$$m_Z = 91.175 \pm 0.021 \text{GeV/c}^2 \tag{13}$$

Multiplying this value with the ratio m_W/m_Z measured by UA2 provided a determination of m_W with a precision of 0.46%:

$$m_W = 80.35 \pm 0.33 \pm 0.17\,\text{GeV/c}^2 \tag{14}$$

in agreement with a direct measurement, $m_W = 79.91 \pm 0.39\,\text{GeV/c}^2$, by the CDF experiment at the Fermilab $p\bar{p}$ collider [19].

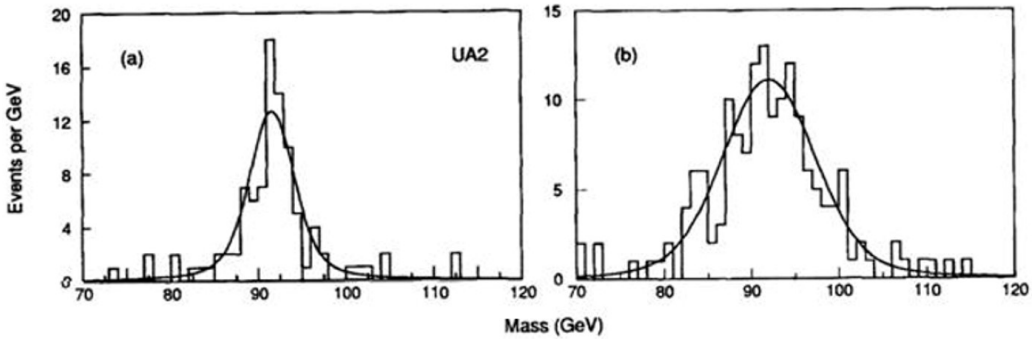

Figure 28. Invariant mass distributions for two $Z \to e^+e^-$ event samples, as measured by UA2 (see text). The curves are best fits to the data using m_Z as a free parameter.

The precise determination of m_W was used to obtain bounds on the top quark mass, for which early direct searches at the CERN and Fermilab $p\bar{p}$ colliders had only provided the lower bound $m_{top} > 89\,\text{GeV/c}^2$ [20–22]. As shown by Veltman [23], within the frame of the Standard Model the value of m_W for fixed m_Z depends quadratically on the mass of the top quark through electroweak radiative corrections from virtual fermion loops (and also, to a much smaller extent, on the mass of the Higgs boson). As illustrated in Figure 29, the UA2 result gave

$$m_{top} = 160^{+50}_{-60}\,\text{GeV/c}^2 \tag{15}$$

suggesting a heavy top quark well before its discovery at the Fermilab $p\bar{p}$ collider with a measured mass $m_{top} = 174 \pm 10 \pm 13\,\text{GeV/c}^2$ [24] (the present world average of all measurements from the experiments at the Fermilab $p\bar{p}$ collider and at the LHC, is $m_{top} = 172.57 \pm 0.29$ GeV/c^2 [25]).

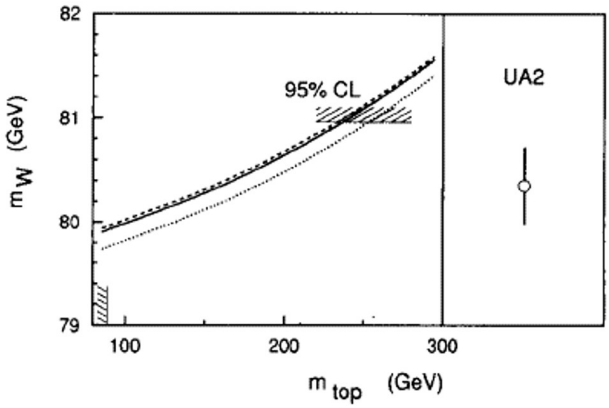

Figure 29. m_W versus m_{top} (curves on the left) and the determination of m_W obtained by combining the precise UA2 measurement of m_W/m_Z with an early precise measurement of m_Z at LEP (the open point with error bar on the right). The curves are the Standard Model predictions for fixed m_Z (as measured at LEP), and for different values of the Higgs boson mass [23]: 50 GeV (dashed curve); 100 GeV (solid curve); and 1000 GeV (dotted curve). Also shown are the 95% confidence level (CL) upper bound $m_{top} < 250\,\text{GeV}$ obtained from the error on m_W, and the lower bound $m_{top} > 89\,\text{GeV}$ from early direct searches at the CERN and Fermilab colliders.

6. Conclusions

The CERN proton-antiproton collider was initially conceived as an experiment to detect the W and Z bosons. Not only it beautifully fulfilled this task, but it also tested the electroweak theory to a level of few percent and provided important verifications of QCD predictions. In the end, it turned out to be a first-class general-purpose accelerator facility with a very rich physics programme, opening the way to the approval of LHC construction.

Conflicts of Interest

The author declares no conflict of interest.

References

1. Rubbia, C.; McIntyre, P.; Cline, D. In Proceedings of the International Neutrino Conference, Aachen, Germany, 8–12 June 1977; p. 683.
2. Haidt, D. The discovery of neutral currents. *Eur. Phys. J. C* **2004**, *34*, 25.
3. Hasert, F.J.; Faissner, H.; Krenz, W.; et al. Search for elastic muon-neutrino electron scattering. *Phys. Lett. B* **1973**, *46*, 121.
4. Hasert, F.J.; Kabe, S.; Krenz, W.; et al. Observation of neutrino-like interactions without muon or electron in the gargamelle neutrino experiment. *Phys. Lett. B* **1973**, *46*, 138.
5. van der Meer, S. *Stochastic Damping of Betatron Oscillations in the ISR*; CERN-ISR-PO 72-31; CERN: Geneva, Switzerland, 1972.
6. Van der Meer, S. Stochastic cooling and the accumulation of antiprotons. *Rev. Mod. Phys.* **1985**, *57*, 689.
7. Carron, G.; Herr, H.; Koziol, H.; et al. Stochastic cooling tests in ice. *Phys. Lett. B* **1978**, *77*, 353.
8. Astbury, A. Calorimeter facilities. *Phys. Scr.* **1981**, *23*, 397.
9. Arnison, G.; Astbury, A.; Aubert, B.; et al. Experimental observation of isolated large transverse energy electrons with associated missing energy at s = 540 GeV. *Phys. Lett. B* **1983**, *122*, 103.
10. Banner, M.; Battiston, R.; Bloch, P.; et al. Observation of single isolated electrons of high transverse momentum in events with missing transverse energy at the CERN. *Phys. Lett. B* **1983**, *122*, 476.
11. Arnison, G.T.; Astbury, A.; Aubert, B.; et al. Experimental observation of lepton pairs of invariant mass around 95 GeV/c^2 at the CERN SPS collider. *Phys. Lett. B* **1983**, *126*, 398.
12. Bagnaia, P.; Banner, M.; Battiston, R.; et al. Evidence for $Z^0 \to e^+e^-$ at the CERN pp collider. *Phys. Lett. B* **1983**, *129*, 130.
13. Albajar, C.; Albrow, M.G.; Allkofer, O.C.; et al. Studies of intermediate vector boson production and decay in UA1 at the CERN proton-antiproton collider. *Z. Phys. C* **1989**, *44*, 15.
14. Albajar, C.; Albrow, M.G.; Allkofer, O.C.; et al. Events with large missing transverse energy at the cern collider: I.W$\to \tau\upsilon$ decay and test of τ μ e universality at $Q^2 = mw^2$. *Phys. Lett. B* **1987**, *185*, 233.
15. Ansari, R.; Bagnaia, P.; Banner, M.; et al. Measurement of the standard model parameters from a study of W and Z bosons. *Phys. Lett. B* **1987**, *186*, 440.
16. Altarelli, G.; Ellis, R.K.; Greco, M.; et al. Vector boson production at colliders: A theoretical reappraisal. *Nucl. Phys. B* **1984**, *246*, 12.
17. Alitti, J.; Ambrosini, G.; Ansari, R.; et al. An improved determination of the ratio of W and Z masses at the CERN pp collider. *Phys. Lett. B* **1992**, *276*, 354.
18. Carter, J. In Proceedings of the Joint International Lepton-Photon Symposium and Europhysics Conference on High Energy Physics, Geneva, Switzerland 25 July–1 August 1991; Volume 2, p. 3.
19. Abe, F.; Amidei, D.; Apollinari, G.; et al. Measurement of the W-boson mass in 1.8-TeV $\bar{p}p$ collisions. *Phys. Rev. D* **1991**, *43*, 2070.
20. Åkesson, T.; Alitti, J.; Ansari, R.; et al. Search for top quark production at the CERN $\bar{p}p$ collider. *Z. Phys. C* **1990**, *46*, 179.
21. Albajar, C.; Albrow, M.G.; Allkofer, O.C.; et al. Search for new heavy quarks in proton-antiproton collisions at $\sqrt{s} = 0.63$ TeV. *Z. Phys. C* **1990**, *48*, 1;
22. Abe, F.; Amidei, D.; Apollinari, G.; et al. Search for the top quark in the reaction $\bar{p}p$ →electron+jets at $\sqrt{s} = 1.8$ TeV. *Phys. Rev. Lett.* **1990**, *64*, 142.
23. Veltman, M. Limit on Mass Differences in the Weinberg Model. *Nucl. Phys. B* **1977**, *123*, 89.
24. Abe, F.; Albrow, M.G.; Amendolia, S.R.; et al. Evidence for top quark production in $\bar{p}p$ collisions at $\sqrt{s} = 1.8$ TeV. *Phys. Rev. D* **1994**, *50*, 2966.
25. Navas, S.; Amsler, C.; Gutsche, T.; et al. Review of Particle Physics. *Phys. Rev. D* **2024**, *110*, 030001.